Visible Light-Induced Polymerization of Monooxiranes and 1,5,7,11-Tetraoxaspiro[5.5]undecanes

CHARLES S. PINZINO,[1] CECIL C. CHAPPELOW,[1] ANDREW J. HOLDER,[2] JASON A. MORRILL,[2] C. DAVID HARRIS,[2] MARTIN D. POWER,[1] J. DAVID EICK[3]

[1] Midwest Research Institute, 425 Volker Boulevard, Kansas City, Missouri 64110-2299

[2] Department of Chemistry, University of Missouri–Kansas City, 5110 Rockhill Road, Kansas City, Missouri 64110

[3] School of Dentistry, Department of Oral Biology, University of Missouri–Kansas City, 650 East 25th Street, Kansas City, Missouri 64108-2975

Received 27 April 2001; accepted 20 September 2001

ABSTRACT: The visible-light photohomopolymerization reactivities of several monofunctional oxiranes were evaluated using photodifferential scanning calorimetry (PDSC). Two oxiranes, styrene oxide and 1-methoxy-2-methyl propylene oxide, were selected for copolymerization reactivity studies with five substituted 1,5,7,11-tetraoxaspiro[5.5]undecanes (TOSUs). Reaction mixtures contained a diaryliodonium salt photoacid initiator and a β-diketone photosensitizer. Experimentally determined reaction enthalpies were compared with calculated theoretical values to assess percent conversion. Relative reactivities were evaluated by comparing induction and exotherm peak maximum times. Results of AM1 semiempirical quantum mechanical calculations of reaction energetics were compared to experimental findings for selected polymerizations. IR spectral changes were consistent with oxirane and TOSU ring opening. The effect of temperature on the photopolymerization reactivity characteristics of glycidyl methylphenyl ether alone and in combination with unsubstituted TOSU was also studied. © 2002 Wiley Periodicals, Inc. J Appl Polym Sci 85: 159–168, 2002

Key words: monooxiranes; epoxides; spiroorthocarbonates; cationic polymerization; photodifferential scanning calorimetry; visible light-induced polymerization; reaction energetics; photopolymerization; ring-opening polymerization; molecular modeling

INTRODUCTION

Since the expansion of spiro-orthocarbonates (SOCs) upon polymerization was first reported by Bailey,[1] their use in dental resins and composites as a way to reduce polymerization shrinkage has been studied.[2,3] In addition, several researchers investigated the copolymerization of SOC/oxirane mixtures using chemical, thermal, UV, and visible light initiation.[4–13] In our research on low shrinkage/reduced stress oxirane-based matrix resins for dental restoratives, we synthesized a number of tetrasubstituted 1, 5, 7, 11-tetraoxaspiro[5.5]undecanes (TOSUs) as potential expandable monomer components. In an attempt to develop a photopolymerization reactivity screening method for these compounds, monooxiranes were chosen as potential coreactants. Both oxiranes and TOSUs are capable of cationic ring-opening polymerization. Visible light photopolymerization can

Correspondence to: J. David Eick.

Contract grant sponsor: NIH/NIDR; contract grant numbers: DE08450; DE096960

Journal of Applied Polymer Science, Vol. 85, 159–168 (2002)

© 2002 Wiley Periodicals, Inc.

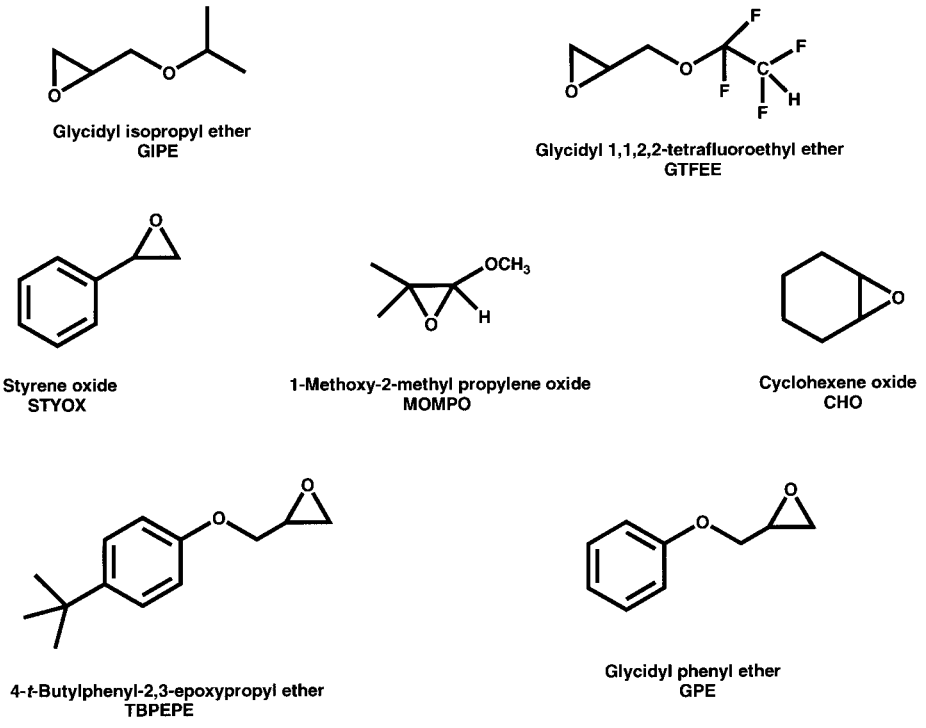

Figure 1 Structures of monooxiranes.

be accomplished using photoacid initiators (e.g., diaryl iodonium salts) in conjunction with β-diketone photosensitizers such as camphorquinone. The relative reactivity of the monofunctional oxiranes, during visible light-initiated homopolymerization, was evaluated in this study using photodifferential scanning calorimetry (PDSC). This technique has been used successfully to study the photopolymerization kinetics of phenyl glycidyl ether.[14] Two oxiranes were selected as comonomers with a series of five TOSUs to determine the relative reactivities of the TOSUs and their effect on the reactivity of the oxiranes.

In addition, semiempirical quantum mechanical methods were used to study reaction mechanisms and energetics for selected polymeriza-

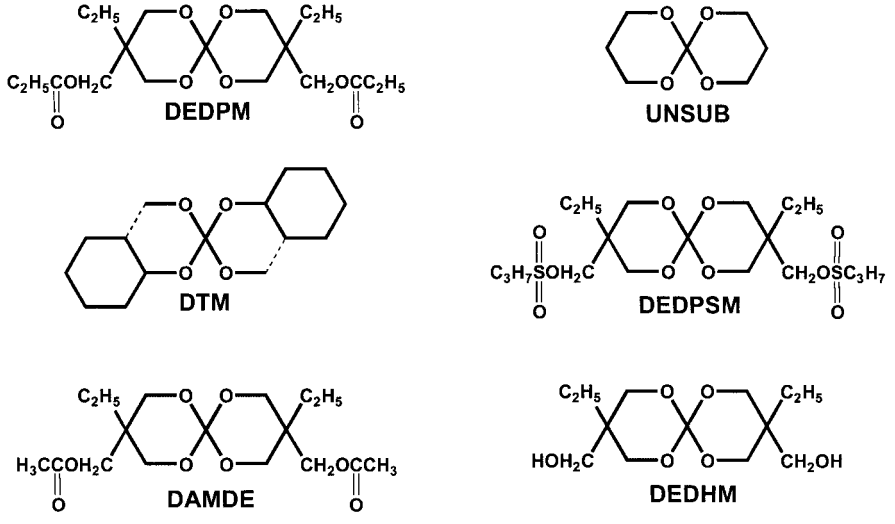

Figure 2 Structures of TOSUs.

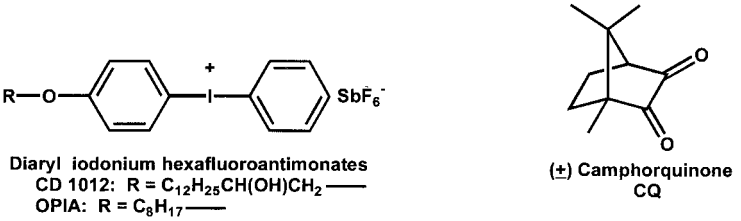

Figure 3 Structures of photoinitiator system components.

tions. These methods have been used previously to study the homopolymerization of spiro-orthocarbonates and other expanding monomer systems.[15,16]

EXPERIMENTAL

Materials

Monofunctional oxiranes were obtained from Aldrich Chemical Co. (Milwaukee, WI) and used as received. They were glycidyl isopropyl ether (GIPE), glycidyl 1,1,2,2-tetrafluoroethyl ether (GTFEE), 4-*tert*-butylphenyl-2,3-epoxypropyl ether (TBPEPE), glycidyl phenyl ether (GPE), glycidyl 2-methylphenyl ether (GMPE), styrene oxide (STYOX), cyclohexene oxide (CHO), and 1-methoxy-2-methyl propylene oxide (MOMPO). Their structures are shown in Figure 1. Six TOSUs, shown in Figure 2, were synthesized at the Midwest Research Institute by reaction of the corresponding diols with tetraethylorthocarbonate in the presence of *p*-toluenesulfonic acid, giving unsubstituted 1,5,7,11-tetraoxaspiro[5.5]undecane[17] [UNSUB], 2,3,8,9-di(tetramethylene)–TOSU[18] [DTM], and 3,9-diethyl-3,9-dihydroxymethyl–TOSU[19] [DEDHM], or by derivatization of the hydroxyl functionality on DEDHM, with acetic anhydride giving 3,9-diacetoxymethyl-3,9-diethyl–TOSU[20] [DAMDE], propionic anhydride giving 3,9-diethyl-3,9-dipropionyloxymethyl–TOSU[20] [DEDPM], or *n*-propylsulfonyl chloride giving 3,9-diethyl-3,9 di(*n*-propylsulfonyloxymethyl–TOSU[20] [DEDPSM]. Characterization by ^{1}H- and ^{13}C-NMR, FTIR, DSC (mp), and elemental analysis was used to confirm the structure. The diaryl iodonium salt photoacid initiators SarCat® CD-1012 (Sartomer, Exton, PA) and (4-octyloxyphenyl)phenyliodonium hexafluorantimonate, OPIA, (479-2092C, GE Silicones, Waterford, NY) and the photosensitizer camphorquinone (Aldrich) were used as received. Structures for the initiatior system components are given in Figure 3.

Methods

Test mixtures for the PDSC reactivity evaluation studies contained oxirane alone or oxirane/TOSU (90/10 mol %), with CD-1012/CQ added at 0.25/0.50 mol %. Photopolymerization characteristics were evaluated using a DuPont/TA Instruments Model 910 DSC equipped with a Model 930 DPC. Samples (14–17 mg) were equilibrated at 37°C prior to irradiation (20 min at 12 mW/cm^2) with the mercury lamp source filtered to eliminate wavelengths below 418 nm. Light intensity entering the sample cell was measured using an International Light IL1400A radiometer with an XRL340A detector. An empty aluminum sample pan (TA Instruments, 900 793.901) was used in the reference position in the DSC cell. A continuous nitrogen purge (40 cc/min) was maintained. The parameters monitored were photopolymerization enthalpy (ΔH_{Photo}); induction time (defined as the time for 1% of the photopolymerization to be complete); and time to the exotherm maximum. Typically, the reproducibility (95% confidence interval) for most PDSC parameter values measured in our laboratory is within ±5–6%. Conversion approximations (%) were calculated for each mixture assuming that all reaction enthalpies resulted from polymerization of the oxirane groups on the monoepoxides: % conversion = $(\Delta H_{\text{Exp}}/\Delta \text{H}_{\text{Theory}}) \times 100$. A value of 94.5 kJ/mol equivalent oxirane[21] was used to calculate theoretical enthalpies.

The effect of the reaction temperature on the photohomopolymerization of GMPE and the photocopolymerization of GMPE/TOSU (70/30 wt %), with OPIA/CQ added at 1.0/0.5 wt %, was also examined using PDSC. Reaction temperatures ranged from 30 to 100°C. A bulk sample (~0.12 g) was prepared in a 9 × 8-mm cylindrical glass mold by irradiating for 12 min at a distance of 2 mm with a 3M XL3000 curing lamp (400–525 nm; 310 mW/cm^2). IR spectra of the mixture were obtained before irradiation and postirradiation

Table I PDSC Photopolymerization Reactivity Parameters and Calculated Theoretical Enthalpies and Conversion (%) for Selected Monooxiranes

Oxirane Monomer	ΔH_{Theory}[a] (J/g)	ΔH_{Exp}[b] (J/g)	Conversion[a] (%)	Induction Time (s)[b]	Exotherm Maximum Time (s)[b]
STYOX	770	651	85	73	118
CHO	938	490	52	61	96
GIPE	795	420	53	49	150
MOMPO	902	322	36	6	9

[a] Theoretical calculated values (see Methods section).
[b] Experimentally determined values (see Methods section).

after a 30-min dark cure using a Perkin–Elmer Model 283 spectrophotometer.

The AM1[22] method was used for reaction energetics calculations as implemented in the program AMPAC with the Graphical User Interface.[23] Ground-state species (reactants and products) were optimized with respect to a minimum-energy geometry and were then characterized by frequency calculations with the requirement that there be no negative eigenvectors present.[24,25] Transition states (TS) for the reactions modeled were located by performing reaction coordinate studies in which the reactant species were forced into proximity to one another along a proposed reaction vector. The maximum in energy geometry resulting from this process was fully optimized (no constraints on geometry) using gradient minimization techniques. The proposed TS was then characterized to assure that one and only one negative eigenvector was present. Further, energy minimizations were carried carried out on slightly distorted TS geometries (one toward the reactant and the other toward the product) to ensure that the located TS actually connected the desired reactants and products. The atomic motions associated with the eigenvector corresponding to the single negative eigenvalue were visually examined using AMPAC's interface to verify that the motions could lead forward to products and backward to reactants. Heats of reaction ($\Delta H_{\text{r}\times\text{n}}$) were computed as the difference between the heat of formation (ΔH_f) of the products and the ΔH_f of a van der Waals complex of the reactant molecules. Enthalpies of activation (ΔH_{act}) were computed as the difference between the TS ΔH_f and the energy of the van der Waals complex of reactant molecules. Entropies (and corresponding Gibbs free energies) were not computed for these processes since bond-breaking and bond-forming processes are characterized by large enthalpy values that dwarf the entropy effects.

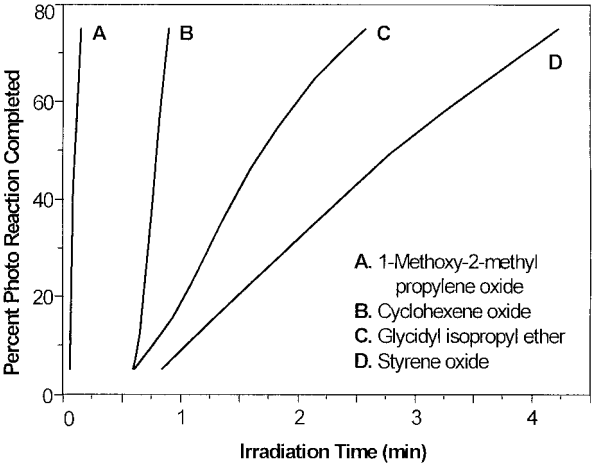

Figure 4 Percent photoconversion versus irradiation time plots for selected monooxiranes.

Table II AM1 Semiempirical Quantum Mechanical Results for the Homopolymerization Reactions for Selected Monooxiranes

Oxirane Monomer	Activation Energy ΔE_{act} (kcal/mol)	Enthalpy of Reaction $\Delta H_{r\times n}$ (kcal/mol)
STYOX	7.6	−29.7
CHO	NAE[a]	−36.0
GIPE	2.4	−13.4
MOMPO	8.4	−23.4

The activation and reaction enthalpies correspond to the activation enthalpy greatest in magnitude for dimerization (between all modes for attack and subsequent ring opening).
[a] NAE, not able to estimate (essentially activationless).

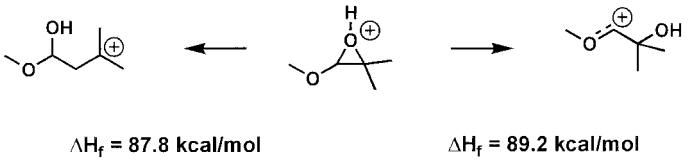

Scheme 1 Possible homopolymerization reaction modes for MOMPO.

RESULTS AND DISCUSSION

Photohomopolymerization reactivity parameters and calculated conversion approximations for STYOX, CHO, GIPE, and MOMPO are given in Table I.

No evidence of photoreaction was detected during 20-min irradiation for GPE, GMPE, TBPEPE, or GTFEE under these reaction conditions. STYOX had the highest percent conversion, while MOMPO had the lowest (85 versus 36%). MOMPO, however, exhibited a much faster reaction rate based on the induction time and the time to the exotherm maximum. A plot of percent photoreaction completed versus time for STYOX, CHO, GIPE, and MOMPO is shown in Figure 4. Based on their different photopolymerization characteristics, STYOX and MOMPO were selected as coreactants for evaluating the relative reactivities of five TOSUs.

Energetics calculations for the homopolymerization of the four monooxiranes that showed significant reactivity under the experimental reaction conditions used are given in Table II. Based on the activation barrier alone, the theoretically predicted order of homopolymerization reactivity for these oxiranes is STYOX < MOMPO < GIPE < CHO. The differences between the energies of activation are small and this makes assignment of reactivity based on this single consideration problematic. When the activation enthalpies are so very close to one another, the Arrhenius "*A*" factors become more important. This is true even for similar reactions proceeding by the same mechanism, as is the case here. If the induction time is used as an experimental reactivity measure, then the order is STYOX < CHO < GIPE < MOMPO. If the time to the exotherm maximum is used, the order is GIPE < STYOX < CHO < MOMPO. In both cases, STYOX is relatively unreactive, a conclusion in agreement with the computational results.

MOMPO has two modes of possible reactions corresponding to formation of a carbocation on each side of the opened epoxide moiety upon protonation. Upon protonation, the oxirane ring can open, giving two possible carbocations: one carbocation is a resonance stabilized form, and the other, a tertiary, with nearly equal enthalpies of formation (Scheme 1).

Calculations indicate that either carbocation form of MOMPO can readily cyclize, halting poly-

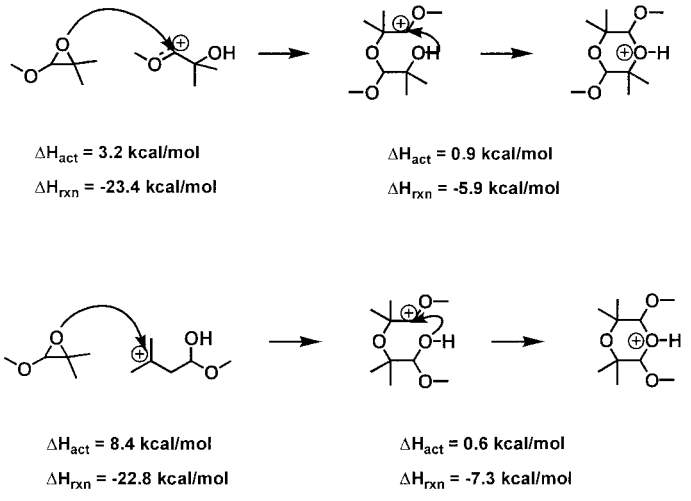

Scheme 2 Cyclizaton of both carbocation forms of MOMPO.

Table III PDSC Photopolymerization Reactivity Parameters and Calculated Theoretical Enthalpies and Conversion Percent for Monooxirane/TOSU (90/10 mol %) Mixtures

Oxirane Monomer	TOSU	ΔH_{Theory}[a] (J/g)	ΔH_{Exp}[b] (J/g)	Conversion[a] (%)	Induction Time (s)[b]	Exotherm Maximum (s)[b]
STYOX	None	770	651	85	73	118
STYOX	DEDHM	618	446	72	68	139
STYOX	DAMDE	584	415	71	113	178
STYOX	DEDPM	573	421	75	129	324
STYOX	DEDPSM	538	489	91	62	134
STYOX	DTM	608	ND	—	—	—
MOMPO	None	902	322	36	6	9
MOMPO	DEDHM	701	230	33	10	16
MOMPO	DAMDE	657	239	36	10	17
MOMPO	DEDPM	643	248	39	14	24
MOMPO	DEDPSM	599	210	35	10	16
MOMPO	DTM	705	145	21	11	26

[a] Theoretical calculated values (see Methods section).
[b] Experimentally determined values (see Methods section).

merization. Activationless ring opening of the attacking monomer immediately follows attack on either ring-opened monomer, giving a resonance-stabilized carbocation. In each case, the alcohol moiety of the dimer can undergo intramolecular attack on the carbocation, giving a protonated dioxane (Scheme 2). The activation barrier for attack on the tertiary carbocation is more than double that for attack on the resonance stabilized carbocation, suggesting that attack on the resonance stabilized form would occur to a greater extent. Note that the conversion percentage (Table I) is based on a theoretical estimate of enthalpy of epoxide polymerization. Since the heat from cyclization is somewhat less than that, this could lead to the low estimated conversion percentage noted for MOMPO in the experimental data.

Photopolymerization reactivity parameters and calculated conversion approximations for STYOX/TOSU and MOMPO/TOSU mixtures are given in Table III. Parameters for STYOX and MOMPO photopolymerizations are repeated for comparative purposes. Conversion percentages for mixtures generally were near those for monoepoxides alone.

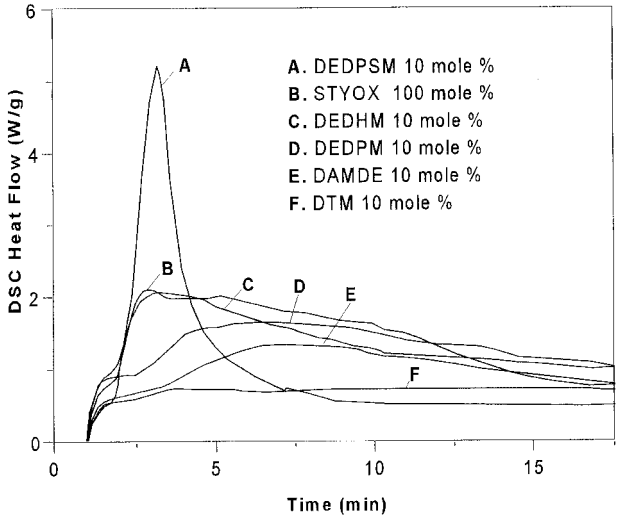

Figure 5 Photopolymerization exotherm profiles for STYOX/TOSU reacton mixtures.

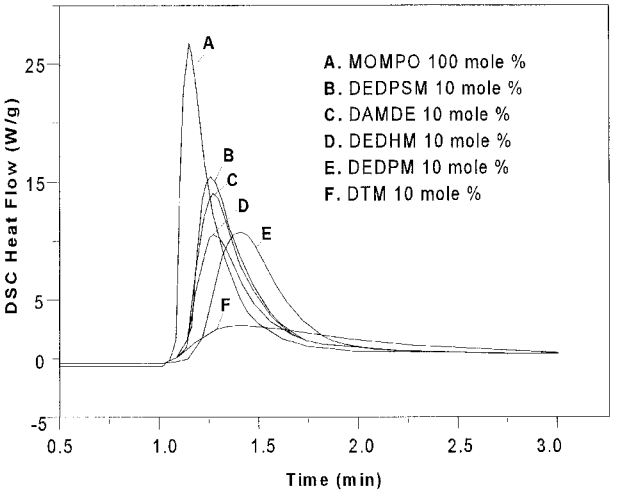

Figure 6 Photopolymerization exotherm profiles for MOMPO/TOSU reaction mixtures.

Table IV AM1 Semiempirical Quantum Mechanical Results for the Reaction Modes of DEDPSM

Reaction Mode	Activation Energy ΔE_{act} (kcal/mol)	Enthalpy of Reaction $\Delta H_{r\times n}$ (kcal/mol)
Homopolymerization	32.6	14.2
Oxirane attack on TOSU ring	31.4	16.0
Oxirane attack on TOSU side chain	17.0	−2.1

PDSC photoreactivity exotherm profiles for STYOX/TOSU and MOMPO/TOSU reaction mixtures are shown in Figures 5 and 6, respectively. Irradiation began at time $t = 1$ min. The STYOX/DEDPSM mixture demonstrated greatly enhanced reactivity, while the STYOX/DTM mixture showed little evidence of reactivity when compared to STYOX alone (Fig. 5). All MOMPO/SOC mixtures showed diminished reactivity and longer peak maximum times when compared to MOMPO alone, with MOMPO/DTM having the lowest reactivity (Fig. 6).

Calculated energetics for three possible reaction modes involving DEDPSM–TOSU are listed in Table IV. The mechanisms for the three modes and resultant products are shown in Scheme 3.

The AM1 calculations on DEDPSM offer a possible explanation for the enhanced reactivity of this monomer when mixed with an oxirane. There are three reasonable possibilities for the reaction of the DEDPSM in the mixture: (1) homopolymerization with other DEDPSM monomers (Scheme 3), high activation barrier and endothermic; (2) copolymerization by reaction with an oxirane to open the TOSU rings (Scheme 4), also high activation barrier and endothermic; and (3) copolymerization by reaction with an oxirane on the side chain at the sulfur center (Scheme 5), much lower barrier and slightly exothermic.

The higher activation barriers and endothermic heats of reaction in the cases of homopolymerization and copolymerization suggest that these reactions will be quite slow compared to reaction at the sulfur center on the side chain. Thus, the explanation of the enhanced apparent reactivity of the DEDPSM compared to the other monomers likely can be traced to the more favorable reaction of oxiranes with the side chain. This reaction is also exothermic, thereby reinforcing the exothermicity of the oxirane polymerization.

It should be noted that interpretation of the PDSC experiments on mixtures must be undertaken with some care. The reason is that the PDSC experiment only measures net heat from a reaction mixture. Thus, if one reactant in a mixture was endothermic while another in the mix-

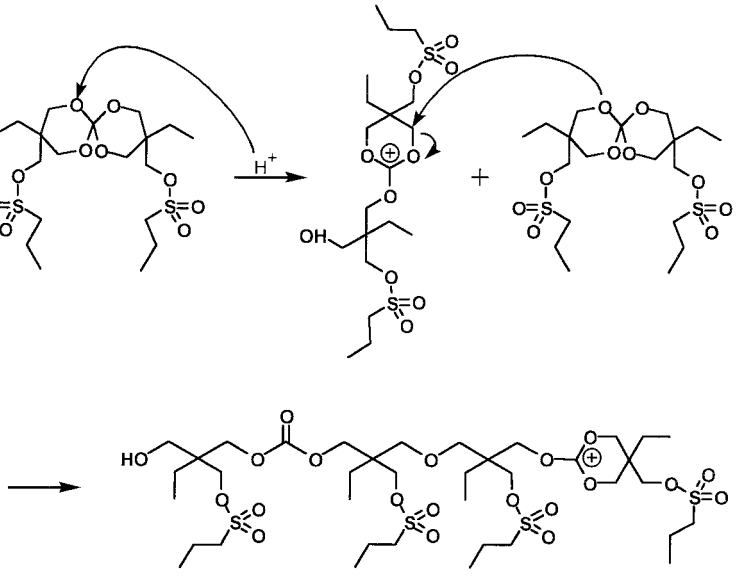

Scheme 3 Homopolymerization of DEDPSM–TOSU.

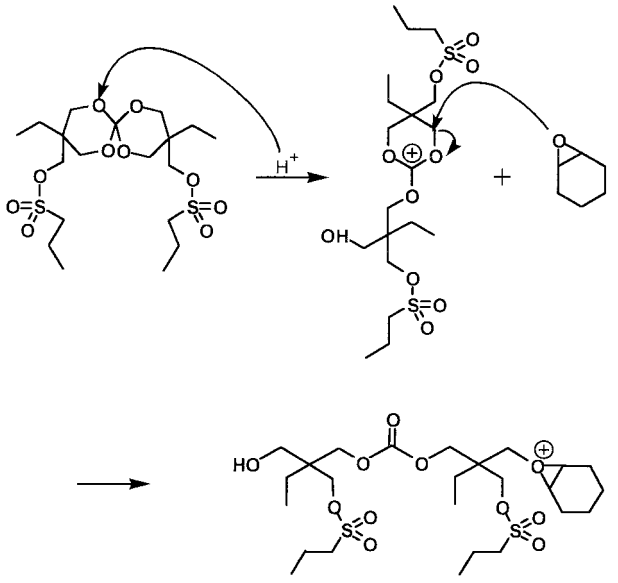

Scheme 4 Copolymerization of DEDPSM–TOSU with an oxirane via TOSU ring opening.

ture was exothermic, the heat absorbed by the endothermic reaction would offset the heat produced by the exothermic reaction. In this case, the net heat produced by the reacting mixture would appear lower than for a mixture where only an exothermic material was reacting in the presence of an unreacting endothermic component. This is the case in the present context since the semiempirical quantum mechanical calculations show that for TOSUs both ring-opening homopolymerization and copolymerization with an oxirane are endothermic[15] while oxirane homopolymerization is very exothermic.[26]

In a PDSC study using GMPE, no homopolymerization photoreaction was observed at temperatures of 30, 60, or 90°C. A reaction mixture containing GMPE/UNSUB (70/30 wt %) showed no photoreactivity at 30°C, but exotherms indicating photoreaction were noted at elevated temperatures (Table V). No reaction exotherm peak was observed when the GMPE/UNSUB mixture was maintained at 90°C for 20 min without irradiation.

Useful information about polymerizates can be obtained by examining IR spectra of reaction mixtures before and after irradiation. Such spectra are presented in Figure 7 for the GMPE/UNSUB system before and after bulk photopolymerization.

In Figure 7(A) (preirradiation), structures of the coreactants are shown, and arrows are used to indicate characteristic spectral bands for purposes of comparison with Figure 7(B) (postirradiation). In Figure 7(B), oxirane ring-opening contributes to the large increase in the —OH band and is evidenced by the diminishment of characteristic epoxide ring bands at ~930 and 780 cm^{-1}. Opening of the TOSU rings also contributes minimally to the increase in the —OH band and is strongly evidenced by the appearance of the large —C═O band at 1750 cm^{-1}. Also, two bands appearing in the IR spectrum of neat UNSUB (not shown) and in the spectrum of the unirradiated GMPE/UNSUB mixture (~1370 and ~1000 cm^{-1}) are greatly diminished or not present in Figure 6(B). Bands characteristic of GMPE (—**C**···**C** doublet at ~1600 cm^{-1} and ortho-sub-

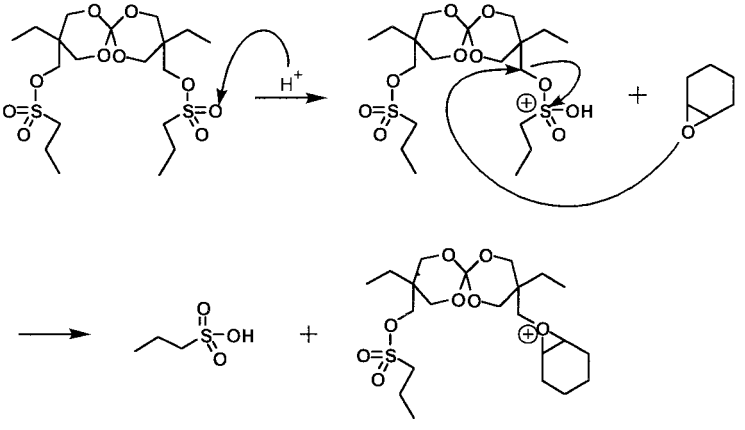

Scheme 5 Copolymerization of DEDPSM–TOSU with an oxirane via reaction with the TOSU side-chain sulfur center.

Table V PDSC Photopolymerization Parameters for GMPE/UNSUB (70/30 wt %) Mixtures at Selected Temperatures

Temperature (°C)	ΔH_{Theory}[a] (J/g)	ΔH_{Exp}[b] (J/g)	Conversion[a] (%)	Induction Time (s)[b]	Time to Exotherm Maximum (s)[b]
45	397	178	45	342	668
60	397	277	70	334	728
90	397	315	79	156	400

[a] Theoretical calculated values (see Methods section).
[b] Experimentally determined values (see Methods section).

stituted aromatic ring band at ~760 cm^{-1}) are present in both spectra.

Characterization of polymerizate products resulting from the photoreactivity evaluations reported here was beyond the scope of this study. Semiempirical quantum mechanical computational techniques have recently been employed to postulate reaction pathways for TOSU homopolymerization and to describe the thermodynamics of potential interactions between TOSUs and oxiranes.[14,15,27–31]

CONCLUSIONS

Monooxirane photohomopolymerizations: Oxirane conversion percentages ranged from 36% (MOMPO) to 85% (STYOX) for four of the eight compounds tested. Four compounds showed no appreciable evidence of reaction under the stated conditions.

Monooxirane/TOSU photocopolymerizations (reactivity screening): Mixtures containing the TOSU DTM exhibited considerably less reactivity than that of other TOSU-containing mixtures. The

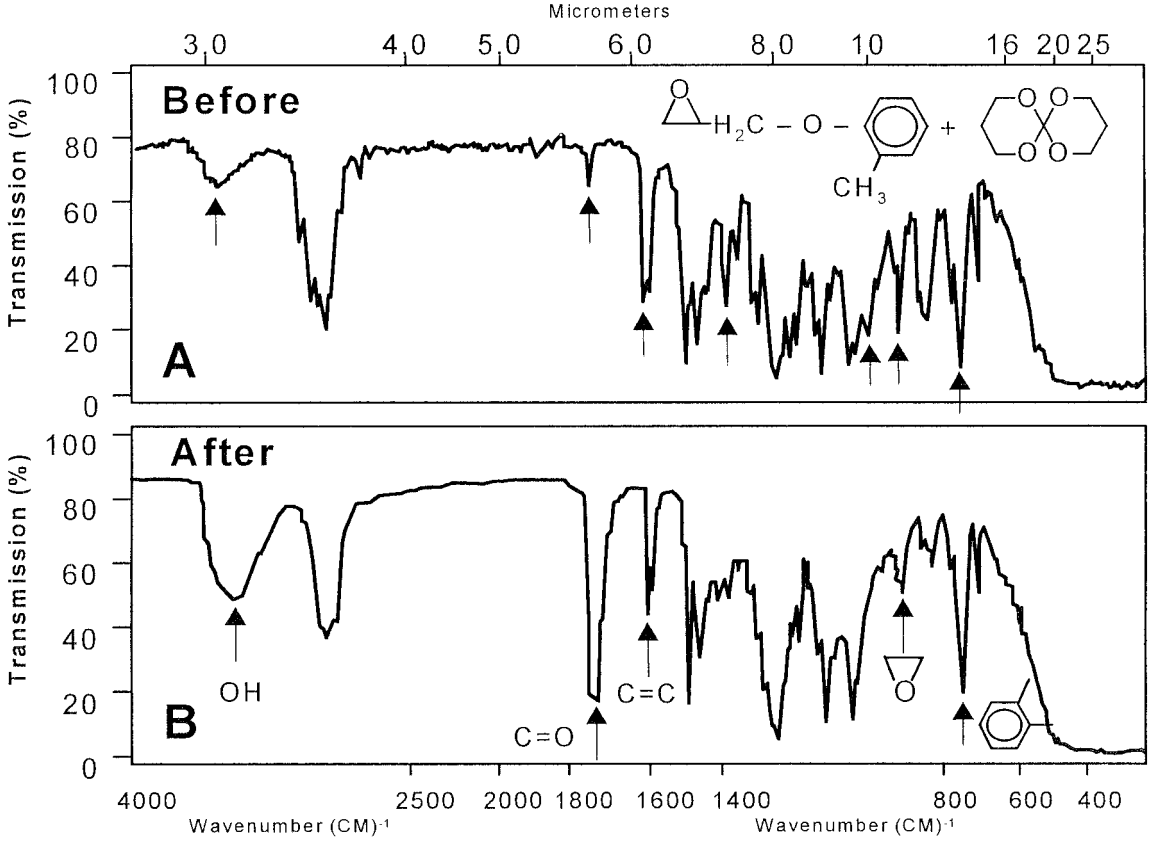

Figure 7 Pre- and postirradiation IR spectra of a GMPE/UNSUB reaction mixture.

STYOX/DEDPSM mixture had a much higher reactivity than that of other STYOX/TOSU reaction mixtures or STYOX alone, perhaps due to preferential attack at the side chain of the TOSU. Measured enthalpies for the reactions were difficult to interpret due to the potential for mixed endothermic and exothermic processes.

Temperature effects: The rate of photopolymerization of monooxirane/TOSU comonomer mixtures can be increased in most cases by elevating the reaction temperature. GMPE/UNSUB mixtures showed increased reactivity as the reaction temperature was increased. It is noteable that GMPE showed little evidence of reactivity during photohomopolymerization attempts at elevated temperatures.

IR analysis: Comparative analysis of IR spectra of monooxirane/TOSU comomomer mixtures before and after irradiation can be used to characterize photopolymerizations. Although IR spectral features indicate evidence of oxirane and spirocyclic ring opening (a prerequisite for copolymerization), no conclusions can be drawn about the composition of resulting photopolymerizates in this study.

This research was supported in part by NIH/NIDR Grant Nos. DE08450 and DE09696.

REFERENCES

1. Bailey, W. J. J Macromol Sci Chem A 1975, 9, 849.
2. Thompson, V. P.; Williams, E. F.; Bailey, W. J. J Dent Res 1979, 58, 1522.
3. Stansbury, J. W.; Bailey, W. J. ACS Symp Prog Biomed Polym 1990, 1988, 133.
4. Bailey, W. J.; Amone, M. J.; Issari, B.; Lin, Y.-N.; No, K.; Pan, C.-Y.; Saigo, K.; Stansbury, J.; Tan, S.-R.; Wu, C.; Yamazaki, N.; Zhou, J. Am Chem Soc Div Polym Mater Prepr 1986, 54, 23.
5. Lim, J. T.; Piggott, M. R.; Bailey, W. J. SAMPE Q 1984, 15(4), 25.
6. Piggott, M. R.; Phshnov, T. Polym Mater Sci Eng 1986, 54, 18.
7. Lam, S. M. Y.; Piggott, M. R. 33rd Int SAMPE Symp 1988, 736.
8. Piggott, M. R.; Lam, P. W. K.; Lim, J. T.; Woo, M. S. Compos Sci Technol 1985, 23, 247.
9. Piggott, M. R.; Woo, M. S. Polym Compos 1986, 7, 182.
10. Piggott, M. R.; Rosen, S. 31st Int SAMPE Symp Exhib 1986, 541.
11. Takata, T.; Endo, T. Polym Prepr Jpn 1988, 37, 241.
12. Eick, J. D.; Byerley, T. J.; Chappell, R. P.; Chen, G. R.; Bowles, C. Q.; Chappelow, C. C. Dent Mater 1993, 9, 123.
13. Chappelow, C. C.; Pinzino, C. S.; Power, M. D.; Eick, J. D. J Dent Res 1997, 76(SI), 40.
14. Ionescu-Vasii, L. L.; Dimonie, M. D.; Abadie, M. J. M. Fr Polym Int 1998, 47, 221.
15. Harris, C. D.; Holder, A. J.; Eick, J. D.; Chappelow, C. C. Theochem 2000, 507, 265–275.
16. Holder, A. J.; White, D. A.; Harris, C. D.; Eick, J. D.; Chappelow, C. C. Theochem, in press.
17. Endo, T.; Okawara, M. Synthesis 1984, 10, 837.
18. Byerley, T. J.; Eick, J. D.; Chen, G. P.; Chappelow, C. C.; Millich, F. Dent Mater 1992, 8, 345.
19. Bailey, W. J.; Sun, R. L.; Katsuki, H.; Endo, T.; Iwama, H.; Tsushima, R.; Saigou, K.; Bitritto, M. ACS Symposium Series 59; American Chemical Society: Washington, DC, 1977; p 38.
20. Chappelow, C. C.; Eick, J. D.; Pinzino, C. S. U.S. Patent 5 808 108, Sept. 15, 1998.
21. Kerr, S. R. III Adhes Age 1996, Aug. 26.
22. Dewar, M. J. S.; Zoebisch, E. G.; Healy, E. F.; Stewart, J. J. P. J Am Chem Soc 1985, 107, 3902–3909.
23. AMPAC with Graphical User Interface; Semichem: Shawnee Mission, KS, 2000. Web: www.semichem.com.
24. McIver, J. W.; Komornicki, A. Chem Phys Lett 1971, 10, 303–306.
25. McIver, J. W.; Komornicki, A. J Am Chem Soc 1972, 94, 2625–2633.
26. Holder, A. J.; Morrill, J. A.; White, D. A.; Eick, J. D.; Chappelow, C. C. Theochem 2000, 507, 63–67.
27. Harris, C. D.; Holder, A. J.; Chappelow, C. C.; Eick, J. D. J Dent Res 1998, 77, 154.
28. White, D. A.; Holder, A. J.; Harris, C. D.; Chappelow, C. C.; Eick, J. D. J Dent Res 1998, 77, 154.
29. Chappelow, C. C.; Pinzino, C. S.; Harris, C. D.; Holder, A. J.; Eick, J. D. J Dent Res 1998, 77, 154.
30. Holder, A. J.; Harris, C. D.; White, D. A.; Chappelow, C. C.; Eick, J. D. J Dent Res 1999, 78, 288.
31. Holder, A. J.; White, D. A.; Harris, C. D.; Chappelow, C. C.; Eick, J. D. J Dent Res 1999, 78, 288.